Ensuring confidence in radionuclide-based sediment chronologies and bioturbation rates

John Crusius[1], Timothy C. Kenna[2]

[1]U.S. Geological Survey

Woods Hole Science Center

Woods Hole, MA 02543

(jcrusius@usgs.gov)

[2]Lamont-Doherty Earth Observatory

of Columbia University

Palisades, NY 10964

(tkenna@ldeo.columbia.edu)

Revised version to Estuarine Coastal and Shelf Science

Abstract

Sedimentary records of naturally occurring and fallout-derived radionuclides are widely used as tools for estimating both the ages of recent sediments and rates of sedimentation and bioturbation. Developing these records to the point of data interpretation requires careful sample collection, processing, analysis and data modeling. In this work, we document a number of potential pitfalls that can impact sediment core records and their interpretation. This paper is not intended as an exhaustive treatment of these potential problems. Rather, the emphasis is on potential problems that are not well documented in the literature, as follows: 1) The mere sampling of sediment cores at a resolution that is too coarse can result in an apparent diffusive mixing of the sedimentary record at rates comparable to diffusive bioturbation rates observed in many locations; 2) ^{210}Pb profiles in slowly accumulating sediments can easily be misinterpreted to be driven by sedimentation, when in fact bioturbation is the dominant control. Multiple isotopes of different half lives and/or origin may help to distinguish between these two possible interpretations; 3) Apparent mixing can occur due simply to numerical artifacts inherent in the finite difference approximations of the advection diffusion equation used to model sedimentation and bioturbation. Model users need to be aware of this potential problem. Solutions to each of these potential pitfalls are offered to ensure the best possible sediment age estimates and/or sedimentation and bioturbation rates can be obtained.

1.0 Introduction

The radionuclides ^{210}Pb and ^{137}Cs are commonly measured in sediments as tools for dating recent sediments and to quantify both sedimentation and bioturbation rates. A flux of ^{210}Pb occurs to the surface of sediments as the result of the decay of ^{222}Rn, a member of the ^{238}U decay series. In shallow fresh and marine sediments, much of the ^{210}Pb results from decay of atmospheric ^{222}Rn, while in deep marine sediments, much of the ^{210}Pb (and ^{222}Rn) is derived from ^{226}Ra in the water column. ^{210}Pb is particle-reactive and quickly sorbs to settling particulate matter. As a consequence of its 22.3-year half-life, ^{210}Pb provides information about sediment ages, accumulation rates, and particle reworking over timescales of roughly 100-150 years (e.g. Robbins, 1978; Appleby, 2001). ^{137}Cs has been distributed globally by atmospheric testing of nuclear weapons. Significant fallout commenced in 1952 and peaked in 1963. This nuclide is also found in surficial sediments because it is also particle reactive. It is used as a chronometer in sediments either by assuming its peak in activity corresponds to the fallout peak in 1963 or its first detection corresponds to the onset of significant fallout in 1952. Where benthic organisms have been active, sedimentary ^{137}Cs distributions can also be used to constrain bioturbation rates and depths (e.g. Cochran, 1985).

The radionuclide ^{228}Th ($t_{1/2}$ = 1.9 y) is a member of the ^{232}Th decay series and is derived from decay of water-column ^{228}Ra. Elevated ^{228}Ra activities are often observed in coastal waters (Yamada and Nozaki, 1986), from which a continuous supply of ^{228}Th is generated. Because Th is particle-reactive, ^{228}Th is rapidly delivered to the seafloor. Excess ^{228}Th (over and above the supporting activities of ^{228}Ra) can develop in coastal

sediments, particularly as the water depth increases along with the inventory of overlying ^{228}Ra. This excess ^{228}Th is another useful tracer of bioturbation depths and rates.

The principles used to infer sediment chronologies and bioturbation rates from these radionuclides are well established. However, generating the best possible interpretation of a dataset of this type requires making wise decisions when collecting and processing sediment samples and when modeling the radionuclide data. There are potential pitfalls in each of these steps that can severely degrade the quality of the final interpretation. This paper is not meant to be an exhaustive review of these potential problems, but instead focuses on how to avoid some of the pitfalls, with an emphasis on issues not well documented in the literature. This paper thus provides insight that will prove useful to the large community of people who use sediment cores and radionuclide-based sediment chronologies for their research, but who are not experts themselves in coring techniques and sediment chronologies. Much of the information presented in this paper will already be known to the research communities focused on studies of bioturbation and recent chronological reconstructions from sediments. We are confident nonetheless, based on numerous interactions with researchers relying on sediment cores for paleoenvironmental and/or surficial process interpretation, that there is a large community for whom the discussion in this paper will prove valuable.

2.0 Methods

The analytical methods used in this work will only be discussed very briefly, as they are well documented in other papers to which we will refer the reader for detail. Sedimentary ^{210}Pb and Th isotope data were determined by dissolving sediment in concentrated nitric, hydrochloric and hydrofluoric acids in a microwave digestion system

followed by alpha counting. ^{210}Pb was plated onto silver disks using the method of Flynn (1968) while Th isotopes were plated using a TTA benzene solution (as described for Pa in Anderson and Fleer, 1982). Supported ^{210}Pb activities were determined from the average total ^{210}Pb activity below the depth at which the activities stop decreasing with depth. Because the excess ^{210}Pb activities are ~30 times higher than this presumed supported ^{210}Pb activity, our interpretations are quite insensitive to this estimate. The excess ^{210}Pb activity was determined by subtracting the supported ^{210}Pb activity from the total ^{210}Pb activity. These data have been previously presented elsewhere (Crusius et al., 1996), but they have not been modeled, which is the focus of this work. Much of this paper, however, focuses on model-based interpretations of idealized data (not these data from the Sea of Japan).

3.0 Modeling radionuclide distribution in sediments

Much of the interpretation in this paper relies upon a model to infer rates of sedimentation and/or bioturbation. In the simplest model version, sedimentation is treated as a process of advection while bioturbation is treated as a process of diffusion (e.g. eq 1) . The radionuclide distribution can be described according to:

$$\frac{\partial \rho A}{\partial t} = \frac{\partial}{\partial z}\left[\frac{D_b \partial \rho A}{\partial z}\right] - s\frac{\partial \rho A}{\partial z} - \lambda \rho A \qquad \text{(Eq. 1)}$$

where

ρ = density of solid phase (cm^3 g^{-1})

A = nuclide activity (dpm g^{-1})

t = time (years)

z = depth (cm)

D_b = diffusive mixing rate (cm^2 yr^{-1})

s = sedimentation rate (cm yr^{-1})

λ = radionuclide decay constant = 0.0311 yr^{-1} for ^{210}Pb and 0.0230 yr^{-1} for ^{137}Cs

This simple treatment of bioturbation provides a reasonable description of data in many cases, and allows quantifying the time-averaged impact of mixing processes using a single parameter, the diffusive mixing coefficient (D_b, cm^2yr^{-1}) (Goldberg and Koide, 1962; Guinasso and Schink, 1975). It is important to bear in mind that treating mixing as a process of diffusion requires making certain assumptions about the depth, symmetry and frequency of sediment mixing (see Boudreau, 1986a and Meysman et al., 2003). For simple, idealized cases there are simple analytical solutions to eq. 1 (e.g. Berger and Heath, 1968; Cochran, 1985; Christensen and Bhunia, 1986) which allow solving for the sedimentation rate, s, and the bioturbation rate, D_b . Again, these solutions will not be repeated here.

For non-idealized and/or non-steady-state conditions there is often no analytical solution to this equation and a numerical sediment mixing model is an excellent tool for quantitative interpretion of radionuclide profiles in sediments. There are many mixing models described in the literature. Some of these utilize diffusive mixing (e.g. Peng et al., 1979; Santschi et al., 1980) while others simulate non-diffusive (e.g. nonlocal) mixing processes. (e.g. Boudreau, 1986b; Robbins, 1986). In this work, we use a numerical model that uses a finite difference approximation of Eq. 1 whose origin dates to Santschi et al., 1980 but has been subsequently modified (Crusius, 1992; Crusius et al, 2004). This model is written in both the C programming language and in Matlab™ and uses the upwind differencing scheme to model sedimentation (as a process of advection)

and the forward time, centered space differencing scheme to model diffusive bioturbation.

4.0 Results and discussion

There are many critical steps between the planning stages of collecting any sedimentary record to the interpretation of high-quality radionuclide-based chronologies and/or sedimentation or bioturbation rates. First, a core must be collected from a region of sediment deposition. These locations can be determined in many cases from predictable patterns of sediment focusing (e.g. sediment accumulates in the deep holes) or from seismic data which show soft mud. Second, the core must be collected in such a way as to preserve the core top. Again, there is a rich literature describing various coring methodologies and how to avoid coring artifacts (e.g. Baxter et al., 1981; Crusius and Anderson, 1991). Once a core has been carefully collected, the core must be sampled properly to ensure a high-resolution record. There are two seemingly routine steps that can potentially have a large impact on the fidelity of the eventual sedimentary record produced: 1) trimming of core edges and 2) sampling at a sufficiently high resolution. It is well known that many sediment coring techniques result in smearing along the core edges (e.g. Chant and Cornett, 1991). Trimming the core edges is necessary to avoid mixing artifacts caused by this process. This issue has been well documented elsewhere (Chant and Cornett, 1991) and will not be repeated here. However, it is not well documented that coarse-resolution sampling of a core can also degrade the temporal resolution of the record and lead to apparent mixing of the sediment.

To demonstrate the effects of sample sectioning alone on resulting down-core profiles, an ideal 1m sediment core was created using the record of annual fallout deposition at New York City

(decay corrected to deposition year) as the source function. Cs-137 deposition was estimated using 1.6x-observed annual ^{90}Sr deposition at New York City (USDOE online database, Larsen, 1982; Cambray et al., 1978). In this paper, we define "ideal" as follows: 1) global fallout deposition is the only source of ^{137}Cs to sediments; 2) there is no mixing; 3) there is no compaction; and 4) there is no wash-in of previously contaminated sediments, or contaminant/sediment focusing. Annual layers in each core profile were constructed using a sedimentation rate of 1.0 cm yr^{-1}. This determined the thickness of each layer and the NYC fallout flux for each year which, in turn, determined the ^{137}Cs activity and inventory in each layer. Once an ideal profile was constructed, sampling at intervals of 1.0, 2.0, 4.0 and 8.0 cm was simulated using Matlab™. When the modeled core was sampled at 1-cm interval from a 1-m sediment core with an accumulation rate of 1.0 cm yr^{-1}, there is in no apparent loss of resolution because the sampling resolution is annual, matching the resolution of the fallout input file. The fact that there is no loss of resolution is apparent in the identical shape of the ^{137}Cs fallout record and sediment profile (Figure 1, first and second rows). When sampling at increasingly coarse resolution, however, two important effects occur, which we address in turn. The first effect is that there is a clear loss of resolution in the record, manifested by a reduced ^{137}Cs maximum and a merging of the 1958 and 1963 peaks (Figure 1 left-hand panels). This effect can be quantified by modeling the effective diffusive mixing rate caused by this process ($D_{sampling}$). $D_{sampling}$ is zero when the core is sampled at 1-cm resolution (again, because both the fallout input function and sediment record have annual resolution). The $D_{sampling}$ estimate is 0.032, 0.32 and 3.0 cm^2yr^{-1} when the core sampling interval is 2, 4 and 8cm (Figure 1, right panels). These rates of effective mixing caused by sampling at coarse resolution are comparable to the diffusive rate of bioturbation often observed in sedimentary records (Olsen et al., 1981; Cochran, 1985; Smith and Schafer, 1984; Thomson et al., 1988; Anderson et al., 1988; Crusius et al., 2004) and suggest that the sampling

strategy alone could have contributed to the apparent mixing observed in some previously published studies. Based on our results, the effects of sampling at coarse resolution are likely to be even more pronounced in areas where sedimentation rates are lower than 1 cm yr^{-1}. A second, fairly obvious, impact of this sort of sampling-induced mixing is that both the depth of initial appearance of ^{137}Cs and the depth of maximum activity become less certain as the sampling resolution coarsens (Figure 1, left panels). It is worth pointing out that, despite the loss of resolution in these records, the ^{137}Cs inventory is preserved in each case. It is also worth pointing out that the size of the sampling interval necessary to resolve the desired features is tracer-specific. In other words, the resolution required to resolve features based on ^{14}C dates would be coarser than that required to resolve features in ^{210}Pb or ^{137}Cs profiles, due to the longer half-life, and longer period of sustained tracer input, for ^{14}C compared to ^{210}Pb and ^{137}Cs.

Another important step towards developing a robust interpretation of sedimentary radionuclide data is to analyze two or more independent chronometers, because the interpretation can be ambiguous or even misleading using only one chronometer. As an example, analyzing the sediment for multiple isotopes can help to resolve whether the coretop is missing, because one cannot necessarily tell based solely on visual inspection, (Crusius and Anderson, 1991), and one cannot tell based solely on ^{210}Pb data, either. A ^{210}Pb profile by itself can only provide an indication of the age of a section of sediment relative to the age of the core top, based on the idea that half the ^{210}Pb decays every 22 years. But if the core top is missing, sediment ages will be biased towards too old an age by an amount equal to the amount of time represented by the missing core top. Achieving agreement between two chronometers (^{210}Pb and ^{137}Cs, for example), or demonstrating the presence of an excess of a short-lived nuclide (^{234}Th ($t_{1/2}$ = 24 d), ^{7}Be

($t_{1/2}$ = 53 d) or ^{228}Th ($t_{1/2}$ = 1.9 y)) can give confidence that there is no material missing from the core top.

Another example demonstrating the value of having multiple tracers of sediment age and bioturbation arises from examination of continental margin ^{210}Pb profiles, which could be driven either by sediment accumulation, bioturbation, or both. There is a common misconception that any ^{210}Pb profile that decreases with depth must reflect sediment accumulation at a rate reflected by the ^{210}Pb slope, rather than reflecting bioturbation. However, in environments with low sedimentation rates, diffusive bioturbation does not necessarily homogenize the ^{210}Pb profile, but rather it results in a ^{210}Pb slope that increases with increasing rates of bioturbation until the ^{210}Pb activity appears constant at a sufficiently rapid rate of mixing (see Figure 2 b). Distinguishing between downward transport of ^{210}Pb due to sediment accumulation and downward transport due to bioturbation requires measurement of independent tracers of sedimentation rate and/or bioturbation rate such as ^{14}C, ^{137}Cs, $^{239+240}$Pu, ^{228}Th, etc.

As an example, we present excess ^{210}Pb data from the continental margin of the Sea of Japan, from a sediment core collected using a multicorer from a water depth of 1473 m (39°50.95'N, 139°10.92'E). This excess ^{210}Pb profile reveals a steeply sloped portion extending from the surface to a depth of ~7 cm, underlain by a more gently sloping region extending to ~11 cm (Figure 2). Examined on its own, these ^{210}Pb data could easily be interpreted to suggest a sedimentation rate at this location of 0.25 cm yr^{-1} at the top of the core, underlain by material deposited at 0.05 cm yr^{-1} (Figure 2 a), perhaps reflecting a recent (anthropogenic) change in sedimentation rate. However, an alternative interpretation could be that there is negligible sedimentation at this site and the

downward transport of ^{210}Pb is due to bioturbation. Indeed, these data can be modeled fairly accurately to suggest a slow sedimentation rate (0.02 cm yr^{-1}) and diffusive bioturbation to a depth of 7 cm at a rate between 0.2 and 2 cm^2y^{-1} (Figure 2 b). Determining which interpretation is correct requires independent information. In this case, we have monospecific foraminiferal AMS ^{14}C dates as well as ^{228}Th data. The ^{14}C-based sedimentation rate is only 0.02 cm yr^{-1}. This is a Holocene average based on a single date within a core spanning 30 kyr; details are presented in Crusius et al. (1999). This ^{14}C-based figure is MUCH lower than would be inferred by assuming the downcore decrease in ^{210}Pb activity is due to sedimentation. Given that the ^{14}C-based accumulation rate reflects a 10,000-year average while the uppermost ^{210}Pb profile would reflect a decadal average, these data do not rule out, of course, that the upper ~7 cm of the record reflects a recent anthropogenic increase in sedimentation. A third independent piece of information settles the issue, however. Excess ^{228}Th (that present in excess of ^{232}Th, its radioactive grandparent), penetrates to a depth of 4-5 cm. These data also are consistent with a bioturbation rate between 0.2 and 2 cm^2yr^{-1} (Figure 2 c). Based on the multi-isotope evidence, therefore, the distribution of all three isotopes in the top 7 cm can be explained by a slow sedimentation rate (0.02 cm yr^{-1}) and bioturbation of the upper ~7 cm of sediment at a rate of 0.2 to 2 cm^2yr^{-1}. These data still do not resolve whether the ^{210}Pb record below ~7 cm truly reflects accumulation at 0.05 cm y^{r-1} (Figure 2 a) or accumulation at 0.02 cm yr^{-1} together with weak bioturbation below 7 cm. The details of this specific example are not important. Rather, the take-home message is that developing a robust interpretation of sedimentary ^{210}Pb data requires information from independent tracers, and possibly interpretation with a sediment-mixing model. In

addition to ^{14}C and ^{228}Th, other independent data that could help resolve these sorts of questions could include fallout tracers such as ^{137}Cs and $^{239+240}Pu$ as well some other independent chronological information (appearance of ragweed pollen, peak in atmospheric Pb fallout, etc). It is important to bear in mind with this type of example that bioturbation can extend to depths of ~30 cm in continental shelf sediments, so bioturbation-driven slopes of excess ^{210}Pb profiles can reach to these depths as well (e.g. Anderson et al., 1988; Crusius et al., 2004), far below the depth of the global average marine sediment mixed layer depth of 10 cm (Boudreau, 1994). It is also important to realize that rates inferred from tracers with different half lives may sometimes be different precisely because they may record processes on different timescales. For example, it has been proposed that short-lived isotopes (^{228}Th) may yield faster rates of bioturbation than long-lived isotopes (^{210}Pb) because the short-lived isotopes may be adsorbed to younger, more labile particles than the longer-lived isotopes (Smith et al., 1993).

Another simple way to examine whether an excess ^{210}Pb record reflects mixing or sedimentation is to plot excess ^{210}Pb versus fallout nuclide data (see Anderson et al., 1988). If there is important chronological information to be gleaned from the excess ^{210}Pb, this plot should show a clear non-zero intercept on the ^{210}Pb axis, because sediments older than 1950 should contain no detectable fallout nuclide while there should still be quantifiable excess ^{210}Pb. On the other hand, if the data are caused by downward mixing, with a negligible contribution from sedimentation, the data will not show a clear intercept on the ^{210}Pb axis and will instead follow a trend through the origin. The methods for quantifying chronological interpretations from ^{210}Pb data are discussed in

detail in other work (e.g. Appleby and Oldfield, 1978; Appleby, 2001) and will not be repeated here.

Numerical models are extremely powerful tools for interpreting sedimentary radionuclide data, as the many papers referred to above help to illustrate. Yet, such models can cause errors in interpretation when used by someone unfamiliar with their idiosynchrosies. Pointing out one important example requires providing some background on the mathematical treatment of many common models. Sediment mixing models utilize numerical techniques (such as finite difference, finite element, etc.) to approximate the equations describing the distribution of these nuclides (e.g. equation 1). These techniques use math no more complicated than division yet they can approximate solutions to differential equations with no analytical solution. In many models (and the model used in this paper), both the advection and diffusion terms are based on Taylor Series approximations of first and second derivatives that allow predicting a future concentration at a given depth from present concentrations at nearby depths and from the depth step (depth resolution) of the model. In this example, we use this type of model to estimate a low mixing rate in a setting where radionuclide transport is dominated by sedimentation, which is modeled here as a process of advection. In the terminology of fluid dynamicists, the Peclet number (Ls/D) is high (L= mixed layer depth (cm); other terms defined in equation 1). It turns out that there is "numerical dispersion" which mixes the modeled radionuclides just as diffusive bioturbation might. This numerical dispersion in the model described here is an artifact of the upwind or backward differencing scheme used for the advection term. Numerical diffusion occurs as a result of the discretization of a continuous system in time and space. For example, consider a

particle moving along a finite difference grid with a spacing of delta z and a time step of delta t. After a particle has been advected along the finite difference grid for a time period (delta t), it must drop onto the closest grid node (the spacing of grid nodes is determined by delta z). At the end of delta t, the particle moves forward if it is more than halfway toward a grid point or backwards if it is less than halfway. As a consequence, the final position of the particle differs slightly from its ideal position, sometimes being slightly farther, and other times not as far, as it would be without such roundoff error. This process is quite similar to random-walk diffusion. This numerical dispersion can actually be quantified as D_{num}, analogous to the diffusive mixing term. This error stems from the truncation of the Taylor series used in the upwind difference approximation of $\frac{\partial C}{\partial z}$. The Taylor theorem states that if the derivatives of a function exist, the function can be represented by a polynomial. From the Taylor series,

$$C_{z-\Delta z} = C_z - \frac{\partial C}{\partial z}\Delta z + \frac{1}{2}\frac{\partial^2 C}{\partial z^2}\Delta z^2 - \frac{1}{3!}\frac{\partial^3 C}{\partial z^3}\Delta z^3 + ... \qquad \text{(Eq. 2)}$$

where

C_z = the concentration at some depth z

Δz = the size of the depth step (cm) between adjacent model grid points

Ignoring the third-order term above and solving for the first derivative yields

$$\frac{\partial C}{\partial z} = -\frac{C_{z-\Delta z} - C_z}{\Delta z} + \frac{\Delta z}{2}\frac{\partial^2 C}{\partial z^2} \qquad \text{(Eq. 3)}$$

We can generate an advective (sedimentation) term as in Eq. 1 by multiplying by –s, as

$$-s\frac{\partial C}{\partial z} = s\frac{C_{z-\Delta z} - C_z}{\Delta z} - \frac{s\Delta z}{2}\frac{\partial^2 C}{\partial z^2} \qquad \text{(Eq. 4)}$$

The upwind difference approximation of this advective term is represented by the right side of equation 4, minus the second term. Note that the second term on the right side has the factor $\frac{s\Delta z}{2}$ multiplied by $\frac{\partial^2 C}{\partial z^2}$ and is thus analogous to the diffusive term in Eq. 1 (in which D is multiplied by $\frac{\partial^2 C}{\partial z^2}$). By ignoring this term, we thus introduce an error that has the same units as diffusion, hence it's called numerical diffusion ($D_{num.}$).

For the steady-state case therefore, (e.g. ^{210}Pb),

$$D_{num.} \approx \frac{s\Delta z}{2} \qquad \text{(Eq. 5)}$$

For the transient state case (i.e. interpretation of fallout nuclides $^{239+240}$Pu and ^{137}Cs),

$$D_{num.} \approx \frac{s\Delta z}{2}(1 - c), \text{ where } c = \frac{s\Delta t}{\Delta z} \qquad \text{(Eq. 6)}$$

where

Δt = the size of the time step (years) between model time points

Equation 6 is from Roache (1972).

In each case above (Eqs. 5 and 6), the numerical dispersion is proportional to the sedimentation rate (s) and to the size of the depth step used (Δz). As a consequence, the impacts of numerical dispersion can be readily observed from plots of model runs with increasingly large depth step (Figure 3a-c). In the ^{137}Cs model simulation, the "double peak" observed in radioactive fallout records in 1958 and 1963 is apparent in the sedimentary record when the depth step is 0.004 cm, but it is gradually eroded as the depth step increases above ~0.01 cm (Figure 3a). Equally important is the fact that the depth of penetration of modeled ^{137}Cs increases from ~14 to ~18 cm as the depth step increases from 0.04 to 0.5 cm (Figure 3b). Since the depth of ^{137}Cs penetration is often

used to suggest a date in the early 1950s when significant atmospheric fallout began, this numerical dispersion would lead to an error in the date assigned to these sediments, merely due to the choice of model depth step. A similar increase in penetration of excess ^{210}Pb (from ~24 to ~28 cm) is apparent when depth step increases from 0.1 to 1 cm (Figure 3c). For this specific case, it's important to minimize the model depth step sufficiently so that it does not bias the sedimentation and age estimates. In our core-sectioning model simulations, $D_{num.}$ was minimized at 5×10^{-7}, 1×10^{-4}, 2.5×10^{-3} and 2.5×10^{-3} cm^2 yr^{-1} for sampling intervals of 1, 2, 4 and 8 cm, respectively. The more important take-home message of this section is that the user of a numerical model must be sufficiently familiar with what the model is doing to ensure appropriate parameters are chosen for the model and insidious problems such as numerical dispersion are avoided.

5.0 Summary and Conclusions

In order to be confident of sediment ages and of sedimentation and bioturbation rates implied by sedimentary radionuclide data, there are a number of important steps to take when collecting and sampling cores and when interpreting and modeling data. The specific steps we document in this work include sectioning sediment cores at sufficiently fine resolution, analyzing the sediment for multiple independent tracers of sedimentation rate and age, and applying an appropriate analytical or numerical model to interpret the data, taking care to avoid numerical artifacts when using numerical models.

Acknowledgements

The authors would like to thank Curtis Olsen, Chuck Holmes, Dan Reed and one anonymous reviewer for constructive comments that improved this manuscript. Thanks also to the U.S. Geological Survey Coastal and Marine Geology Program, the Andrew F. Mellon Foundation, the Earth Institute Postdoctoral Fellowship Program at Columbia University, and the National Science Foundation for funding. This is LDEO contribution XXXX.

References

Anderson, R.F. and Fleer, A.P., 1982. Determination of natural actinides and plutonium in marine particulate material. *Anal. Chem.*, **54**: 1142-1147.

Anderson, R.F., Bopp, R.F., Buesseler, K.O. and Biscaye, P.E., 1988. Mixing of particles and organic constituents in sediments from the continental shelf and slope off Cape Cod: SEEP-I results. Cont. Shelf Res., 8: 925-946.

Appleby, P.G. and Oldfield, F., 1978. The calculation of ^{210}Pb dates assuming a constant rate of supply of unsupported ^{210}Pb to the sediment. Catena, 5: 1-8.

Appleby, P.G., 2001. Chronostratigraphic techniques in recent sediments. In: W.M. Last and J.P. Smol (Editors), Tracking Environmental Change Using Lake Sediments Volume 1: Basin Analysis, Coring, and Chronological Techniques. Kluwer Academic, pp. 171-203.

Baxter, M.S., Farmer, J.G., McKinley, I.G., Swan, D.S. and Jack, W., 1981. Evidence of the unsuitability of gravity coring for collecting sediment in pollution and sedimentation rate studies. E S and T, 15: 843-846.

Berger, W.H. and Heath, G.R., 1968. Vertical mixing in pelagic sediments. J. Mar. Res., 26: 134-143.

Boudreau, B.P., 1986a. Mathematics of tracer mixing in sediments: I. Spatially-dependent, diffusive mixing. American Journal of Science, 286: 161-198.

Boudreau, B.P., 1986b. Mathematics of tracer mixing in sediments: II. Nonlocal mixing

and biological conveyor-belt phenomena. American Journal of Science, 268: 199-238.

Boudreau, B.P., 1994. Is Burial Velocity A Master Parameter For Bioturbation. Geochimica Et Cosmochimica Acta, 58(4): 1243-1249.

Cambray, R.S., Fisher, E.M.R. and Playfort, K., 1978. Radioactive fallout in air and rain; results to the end of 1977. AERE-R-9016.

Chant, L.A. and Cornett, R.J., 1991. Smearing Of Gravity Core Profiles In Soft Sediments. Limnology And Oceanography, 36(7): 1492-1498.

Christensen, E.R. and Bhunia, P.K., 1986. Modeling radiotracers in sediments; comparison with observations in lakes Huron and Michigan. Journal of Geophysical Research. C. Oceans and Atmospheres, 91(7): 8559-8571.

Cochran, J.K., 1985. Particle mixing rates in sediments of the eastern equatorial Pacific: Evidence from ^{210}Pb, $^{239+240}$Pu and ^{137}Cs distributions at MANOP sites. Geochimica et Cosmochimica Acta, 49: 1195-1210.

Crusius, J. and Anderson, R.F., 1991. Core Compression And Surficial Sediment Loss Of Lake-Sediments Of High Porosity Caused By Gravity Coring. Limnology And Oceanography, 36(5): 1021-1030.

Crusius, J., 1992. Evaluating the mobility of ^{137}Cs, $^{239+240}$Pu and ^{210}Pb from their distributions in laminated sediments. Ph.D. Thesis, Columbia University, New York, 253 pp.

Crusius, J., Calvert, S., Pedersen, T. and Sage, D., 1996. Rhenium and molybdenum enrichments in sediments as indicators of oxic, suboxic and sulfidic conditions of deposition. Earth And Planetary Science Letters, 145(1-4): 65-78.

Crusius, J., Pedersen, T.F., Calvert, S.E., Cowie, G.L. and Oba, T., 1999. A 36 kyr geochemical record from the Sea of Japan of organic matter flux variations and changes in intermediate water oxygen concentrations. Paleoceanogr., 14: 248-259.

Crusius, J., Bothner, M. and Sommerfield, C.K., 2004. Bioturbation depths, rates and processes in Massachusetts Bay sediments inferred from modeling of ^{210}Pb and $^{239+240}$Pu profiles. Est. Coast and Shelf Sci., 61(4): 643-655.

Flynn, W.W., 1968. The determination of low levels of polonium-210 in environmental materials. Analytica Chimica Acta, 43: 221-227.

Goldberg, E.D. and Koide, M., 1962. Geochronological studies of deep sea sediments by the ionium/thorium method. Geochimica et Cosmochimica Acta, 26: 417-450.

Guinasso, N.L., Jr. and Schink, D.R., 1975. Quantitative estimates of biological mixing rates in abyssal sediments. Journal of Geophysical Research, 80(21): 3032-3043.

Larsen, R.J., 1982. Quarterly Sr-90 Deposition at World Land Sites. USDOE Report EML-412.

Meysman, F.J.R., Boudreau, B.P. and Middelburg, J.J., 2003. Relations between local, nonlocal, discrete and continuous models of bioturbation. Journal Of Marine Research, 61(3): 391-410.

Olsen, C.R., Simpson, H.J., Peng, T.-H., Bopp, R.F. and Trier, R.M., 1981. Sediment

mixing and accumulation rate effects on radionuclide depth profiles in Hudson estuary sediments. J. Geophys. Res., 86: 11020-11028.

Peng, T.-H., Broecker, W.S. and Berger, W.H., 1979. Rates of benthic mixing in deep-sea sediment as determined by radioactive tracers. Quat. Res., 11: 141-149.

Roache, P.J., 1972. On artificial viscosity. J. Comput. Phys., 10: 351-365.

Robbins, J.A., 1978. Geochemical and geophysical applications of radioactive lead. In: J.O. Nriagu (Editor), The biogeochemistry of lead in the environment. Elsevier, pp. 285-393.

Robbins, J.A., 1986. A model for particle-selective transport of tracers in sediments with conveyor belt deposit feeders. J. Geophys. Res., 91: 8542-8558.

Santschi, P., H., Li, Y.-H., Bell, J.J., Trier, R.M. and Kawtaluk, K., 1980. Pu in coastal marine environments. Earth and Planet. Sci. Lett., 51: 248-265.

Smith, J.N. and Schafer, C.T., 1984. Bioturbation processes in continental slope and rise sediments delineated by Pb-210, microfossil and textural indicators. J. Mar. Res., 42: 1117-1145.

Smith, C.R., Pope, R.H., DeMaster, D.J. and Magaard, L., 1993. Age-dependent mixing of deep-sea sediments. Geochimica et Cosmochimica Acta, 57: 1473-1488.

Thomson, J., Colley, S. and Weaver, P.P.E., 1988. Bioturbation into a recently emplaced deep-sea turbidite surface as revealed by ^{210}Pb, ^{230}Th and planktonic foraminifera distributions. Earth and Planetary Science Letters, 90: 157-173.

Yamada, M. and Nozaki, Y., 1986. Radium isotopes in coastal and open ocean surface waters of the western North Pacific. Marine Chemistry, 19(4): 379-389.

Figure captions

Figure 1: Effects of different core sectioning intervals on ^{137}Cs profile and sediment mixing model results. Fallout record for New York City (top left) used as ^{137}Cs input for all model runs (see text). Left-hand panels (step plots) show results of sampling an ideal sediment column accumulating at 1 cm yr^{-1} at increasingly coarse intervals. Dashed gray line indicates the "true" depth of the ^{137}Cs maximum. Right-hand panels show plots with the average activity for the sampling interval plotted at the midpoint (black lines with open circles); dark gray lines show model results and calculated mixing rates. Note error bars represent an assumed uncertainty of 10 percent with respect to ^{137}Cs activities.

Figure 2: a) Excess ^{210}Pb data (squares) from MC8B from the continental margin of the Japan Sea (39°50.95'N, 139°10.92'E, 1473 m), and model fits to the data assuming the ^{210}Pb profiles are driven by sedimentation only (no bioturbation) at rates of 0.25 cm yr^{-1} (solid line) and 0.05 cm yr^{-1} (dashed line). Also shown is the trend that would be predicted based on the measured ^{14}C-inferred sedimentation rate of 0.021 cm yr^{-1} (dotted line). b) Model fits to the excess ^{210}Pb data (squares) assuming the ^{14}C-inferred sedimentation rate (0.021 cm yr^{-1}), with diffusive mixing rates ranging from 0.02-2 cm^2 yr^{-1}; c) Modeled profile of ^{228}Th/^{232}Th (activity ratio) assuming the ^{14}C-inferred sedimentation rate and the diffusive bioturbation rates of 0.2 and 2 cm^2 yr^{-1}.

Figure 3: Numerical dispersion in modeled ^{137}Cs and ^{210}Pb profiles. a) Modeled ^{137}Cs profiles varying only the model depth step. Note that the numerical dispersion increases with increasing depth step (thin solid line, 0.004 cm; dashed line, 0.01 cm; dotted line, 0.1 cm; thick line with diamonds, 0.5 cm); b) Expansion of 3a showing the region at the base of ^{137}Cs penetration; c) Modeled ^{210}Pb profile with varying depth step (thin solid line,

analytical solution; dashed line, depth step = 0.1 cm; dotted line, 0.3 cm; thick line with diamonds, 1 cm)

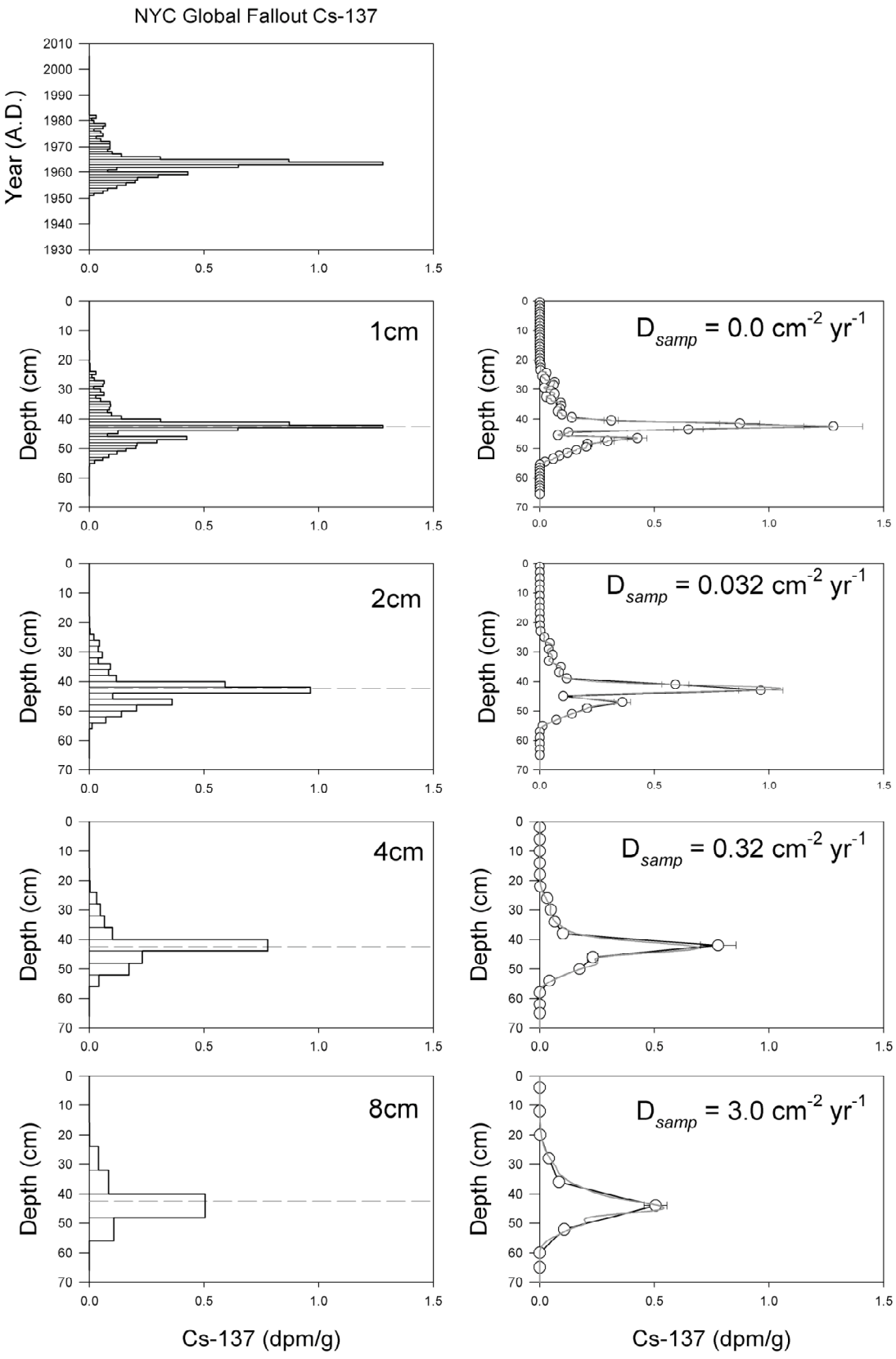
NYC Global Fallout Cs-137
Year (A.D.)
2010
2000
1990
1980
1970
1960
1950
1940
1930
0.0
0.5
1.0
1.5
Depth (cm)
0
10
20
30
40
50
60
70
1cm
2cm
4cm
8cm
D_{samp} = 0.0 cm^{-2} yr^{-1}
D_{samp} = 0.032 cm^{-2} yr^{-1}
D_{samp} = 0.32 cm^{-2} yr^{-1}
D_{samp} = 3.0 cm^{-2} yr^{-1}
Cs-137 (dpm/g)
Cs-137 (dpm/g)

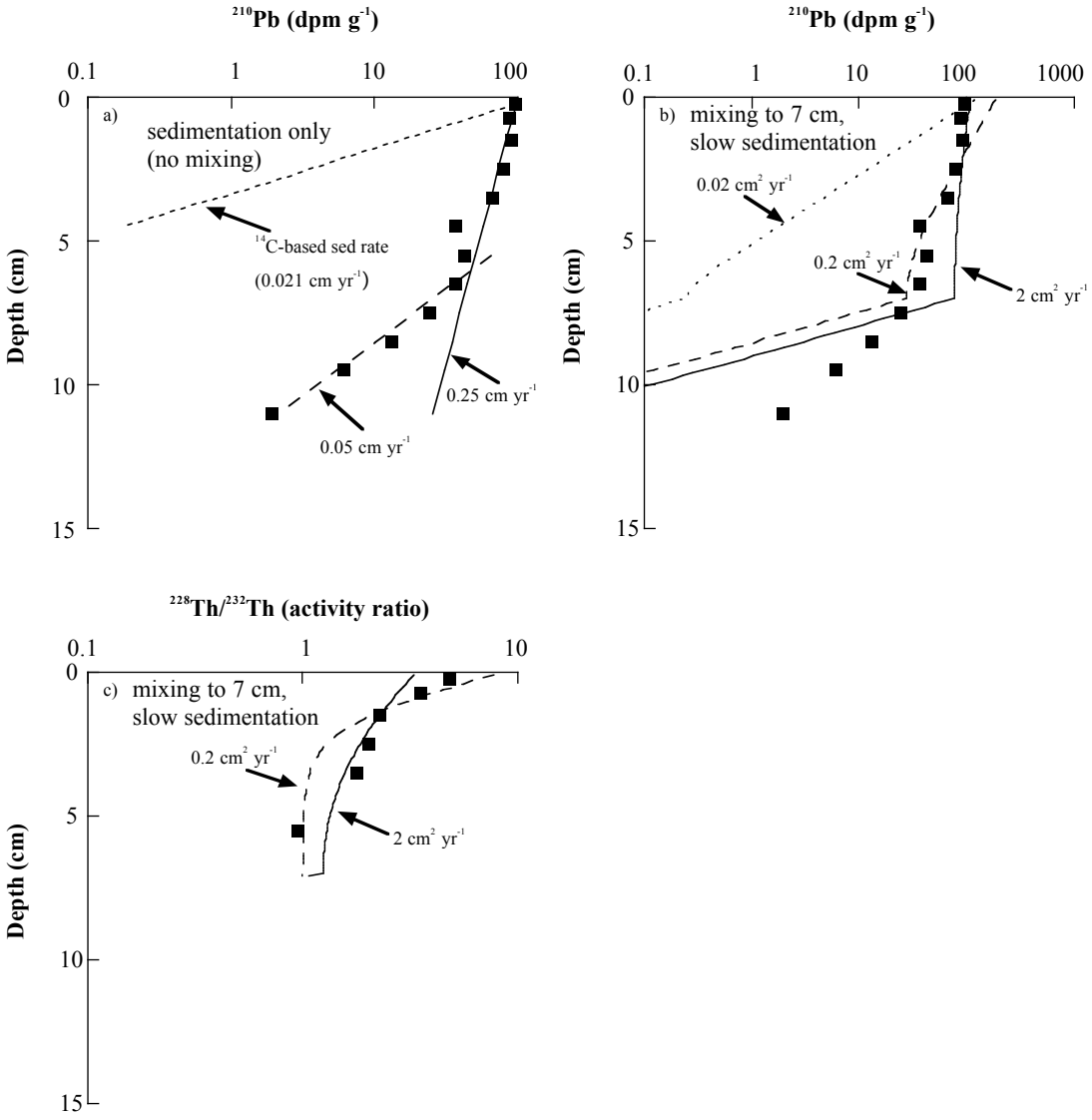

Figure 2 Crusius and Kenna

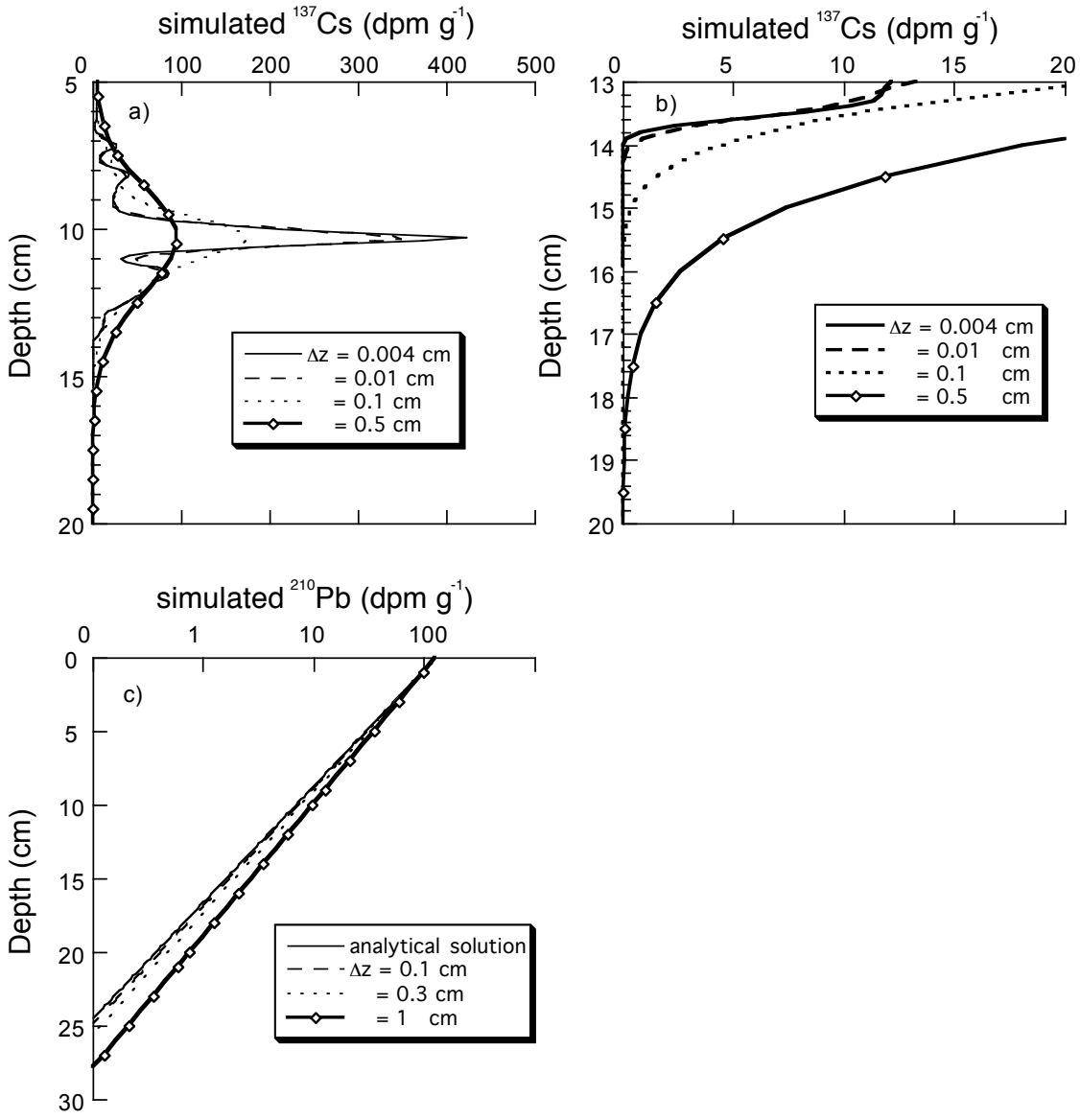

Figure 3 Crusius and Kenna